



Title	Optimal Scheduling With Vehicle-to-Grid Regulation Service
Author(s)	Lin, J; Leung, KC; Li, VOK
Citation	IEEE Internet of Things Journal, 2014, v. 1, p. 556-569
Issued Date	2014
URL	http://hdl.handle.net/10722/217036
Rights	IEEE Internet of Things Journal. Copyright © IEEE.

Optimal Scheduling of Vehicle-to-Grid Energy and Ancillary Services

Eric Sortomme, *Student Member, IEEE*, and Mohamed A. El-Sharkawi, *Fellow, IEEE*

Abstract—Vehicle-to-grid (V2G), the provision of energy and ancillary services from an electric vehicle (EV) to the grid, has the potential to offer financial benefits to EV owners and system benefits to utilities. In this work a V2G algorithm is developed to optimize energy and ancillary services scheduling. The ancillary services considered are load regulation and spinning reserves. The algorithm is developed to be used by an aggregator, which may be a utility or a third party. This algorithm maximizes profits to the aggregator while providing additional system flexibility and peak load shaving to the utility and low costs of EV charging to the customer. The formulation also takes into account unplanned EV departures during the contract periods and compensates accordingly. Simulations using a hypothetical group of 10 000 commuter EVs in the ERCOT system using different battery replacement costs demonstrate these significant benefits.

Index Terms—Aggregator, demand response, profit optimization, regulation, spinning reserves, vehicle-to-grid (V2G).

I. NOMENCLATURE

$BatC_i$	The battery replacement cost of the i^{th} EV	Ex_D	Expected percentage of regulation down capacity dispatched each hour.
C	Aggregator costs.	Ex_R	Expected percentage of responsive reserve capacity dispatched each hour.
$Comp_i(t)$	Compensation factor of the i^{th} EV to account for unplanned departures.	Ex_U	Expected percentage of regulation up capacity dispatched each hour.
CR_i	Charge remaining to be supplied to the i^{th} EV.	$EVPer(t)$	Expected percentage of the EVs remaining to perform V2G at hour t .
DC_i	Degradation cost to the battery from discharging plus a compensation amount to ensure the aggregator cannot take advantage of charging and discharging efficiencies to charge the customer more.	FP_i	Final power draw of the i^{th} EV combining the effects of regulation and responsive reserves.
$Deg_i(t)$	An epigraph variable to model battery degradation.	In	Income of the aggregator.
$Dep_i(t)$	Probability that the i^{th} EV will depart unexpectedly in hour t .	$L(t)$	System net load (load minus renewables) at time t .
$E[\]$	Expected value function	MC_i	Maximum charge capacity of the i^{th} EV.
Ef_i	Efficiency of the i^{th} EV's battery charger.	Mk	The price of energy charged to the customer.
		$MnAP_i$	Minimum additional power draw of the i^{th} EV.
		Mn_L	Minimum day-ahead forecasted net load.
		$MP_i(t)$	Maximum possible power draw of i^{th} EV at time t . If the EV is not plugged in, this value is 0.
		$MxAP_i$	Maximum additional power draw of the i^{th} EV.
		Mx_L	Maximum day-ahead forecasted net load.
		$P(t)$	Energy price at time t .
		PD_i	Power draw of the battery of the i^{th} EV.
		POP_i	Preferred operating point of the i^{th} EV.
		$Pr[\]$	Probability of dispatch for ancillary services
		$PRD(t)$	Forecasted price of regulation down for time t .
		$PRR(t)$	Forecasted price of responsive reserves for time t .
		$PRU(t)$	Forecasted price of regulation up for time t .
		R_D	Regulation down capacity of the aggregator.
		R_R	Responsive reserve capacity of the aggregator.

Manuscript received February 21, 2011; revised June 23, 2011; accepted July 29, 2011. Date of publication September 19, 2011; date of current version February 23, 2012. Paper no. TSG-00056-2011.

The authors are with the Department of Electrical Engineering, University of Washington, Seattle, WA 98195 USA (email: eric.sortomme@gmail.com, melshark@u.washington.edu).

Color versions of one or more of the figures in this paper are available online at <http://ieeexplore.ieee.org>.

Digital Object Identifier 10.1109/TSG.2011.2164099

RRS	Responsive reserve signal provided to the aggregator.
RS	System regulation signal provided to the aggregator.
$RsRP_i$	Reduction in power draw available for spinning reserves of the i^{th} EV.
R_U	Regulation up capacity of the aggregator
SOC_i	State of charge of the i^{th} EV battery
$SOC_{I,i}$	Initial state of charge of the i^{th} EV
T	The ending time of the daily scheduling.
$Trip_i(time)$	The reduction in SOC that results from the evening commute trip home on a weekday and the second daily trip on the weekend. In the formulation, when looking ahead if the commute will occur after the hour considered, $Trip_i(time)$ is 0. If the trip occurs before the hour considered, $Trip_i(time)$ is the energy used on the trip. If the trip has already occurred, $Trip_i(time) = 0$.
$T_{trip,i}$	Time that the i^{th} EV makes its second trip of the day. On a weekday this is the commute from work to home. On the weekend this is simply the second excursion which ends when the EV returns home.

II. INTRODUCTION

INTEGRATING large numbers of electric vehicles (EVs) into the power grid while simultaneously reducing their impacts and those of uncontrollable renewable energy sources is a major goal of vehicle-to-grid (V2G) systems [1]. V2G is defined as the provision of energy and ancillary services, such as regulation or spinning reserves, from an EV to the grid. This can be accomplished by discharging energy through bidirectional power flow, or through charge rate modulation with unidirectional power flow [1]–[3]. Through V2G, EV owners can produce revenue while their cars are parked which can provide valuable economic incentives for EV ownership. Utilities can also benefit significantly from V2G by having increased system flexibility as well as energy storage for intermittent renewable energy sources such as wind. In order to participate in energy markets, the V2G capabilities of many EVs are combined by aggregators and then bid into the appropriate markets [4]–[9]. An aggregator may be the utility into which the EVs are plugged or a third party business.

Though it has been speculated that unidirectional V2G will be implemented first [3], it has several limitations. One of which is that the regulation and reserves capacities bid with unidirectional V2G are significantly less than those that can be bid in bidirectional V2G [10]. Unidirectional V2G also cannot provide the system with the energy stored in the EV batteries.

Recently there has been a flurry of activity with respect to V2G. It has been shown that EVs can be dispatched to follow

system regulation signals [11], [12]. Simulations have shown that the EVs acting as smart storage can provide fast and accurate responses for frequency regulation and spinning reserves to aid in the integration of wind and solar power [13]–[15]. These studies, however, did not consider market conditions in determining the amount of regulation services to be provided and there was no optimization of the V2G assets. Another important study looked at the potential to provide V2G regulation and spinning reserves based on EV availability [16]. This study looked at the available EVs to perform V2G both from monthly averages and using Monte Carlo simulations. This study also did not perform any optimization of the V2G assets.

Several studies have looked at optimization of V2G assets. In [3], an optimal bidding formulation for EVs performing regulation up and down with only unidirectional power flow was developed. The simulations were performed on a simulated market with constant prices of regulation services over the study year. In [7], an optimal charging sequence for EVs selling only regulation is formulated. This formulation does not consider bulk discharging for a source of income and bids symmetric capacities of regulation up and down. It also assumes that periods of charging are decoupled from periods of performing regulation, that is, the POP is always zero when performing regulation. In [17], smart charging optimization without V2G and optimized V2G with only regulation is formulated. This formulation did not consider the change in battery SOC from dispatch of regulating power through symmetric bidding of regulation up and down. It also does not consider bulk discharge of the battery during peak prices.

In this work the problem of optimal simultaneous bidding of V2G energy and ancillary services for aggregator profit maximization is formulated. The aggregator costs and revenues are structured such that maximum aggregator profits will be associated with maximum system benefits and low customer costs. This formulation relies on most probable EV driving forecasts and the compensation required for unexpected deviations from the forecasts. Battery degradation costs associated with additional cycling, as described in [18], [19], are also accounted for. The main contributions of this formulation are:

- To simultaneously optimize bidding of V2G:
 - Energy;
 - Regulation up;
 - Regulation down;
 - Spinning reserves;
- The formulation of the problem as a linear program which can be quickly and efficiently solved for large groups of EVs.

This formulation considers the selling of bulk energy and spinning reserves which were not considered in [3], [7], and [17]. It also allows asymmetric bidding of regulation up and down as well as a biased POP in either direction, which were not considered in [7] and [17]. Additionally, this formulation allows bidding of capacities of energy and services less than the available EV battery capacities. Unlike [17], the power losses and gains due to dispatch of ancillary services are considered in the formulation since they cannot be neglected with asymmetric bidding. The formulation also considers EV driving behavior with unexpected departures during scheduling periods which is essential for an aggregator [9], [16].

Additionally, algorithms for EV dispatch of regulation and spinning reserves are developed, which were not considered in [7] and [17]. These algorithms modulate the charging and discharging rates of a single EV around a set point to follow the regulation and responsive reserves signals received from the system operator.

To test the efficacy of the algorithms, they are simulated using hypothetical group of 10 000 commuter EVs in Houston, TX. A group of 10 000 allows for determining the power per vehicle with high certainty [16]. These simulations are over a three-month period using the actual historical market data with different EV battery replacement costs. Simulation results show that even though the costs associated with battery degradation are considerable, the aggregator receives significant profits while keeping consumer costs for energy extremely low. In addition to the extra flexibility provided, system peak load is generally reduced due to the energy discharged from the batteries.

III. PROBLEM FORMULATION

Optimization of V2G assets will be performed by aggregators because aggregators will provide the interface between EVs and the energy markets [5], whether the aggregator is a utility or a third party. In this formulation, aggregator revenue comes from three sources as shown in (1). These sources are a fixed rate on energy delivered to the EV, the revenues from selling regulation and responsive reserves (the term for spinning reserves in the ERCOT market) capacity, and the revenues from selling energy. Since the dispatch of energy according to the regulation and reserves signals cannot be known in advance, the expected value of the final power draw is used when calculating the income. The expected value of power draw is a function of the POP in addition to the expected values of regulation down, regulation up, and responsive reserves. The calculation of the expected final power draw is given in (2)–(5).

$$\begin{aligned}
 In = & \sum_t (P_{RU}(t) \cdot R_U(t) + P_{RD}(t) \cdot R_D(t) \\
 & + P_{RR}(t) \cdot R_R(t)) \\
 & + Mk \sum_i \sum_t (E [FP_i(t)]) \\
 & + \sum_i \sum_t (E [FP_i(t)] \cdot P(t)) \text{ if } E [FP_i(t)] \leq 0
 \end{aligned} \quad (1)$$

$$\begin{aligned}
 E [FP_i(t)] = & MxAP_i(t) \cdot Ex_D + POP_i(t) \\
 & - MnAP_i(t) \cdot Ex_U - RsRP_i(t) \cdot Ex_R
 \end{aligned} \quad (2)$$

$$Ex_D = \frac{\int_{RS_{\min}}^0 RS \cdot Pr[RS] \cdot dRS}{\int_{RS_{\min}}^0 RS \cdot dRS} \quad (3)$$

$$Ex_U = \frac{\int_0^{RS_{\max}} RS \cdot Pr[RS] \cdot dRS}{\int_0^{RS_{\max}} RS \cdot dRS} \quad (4)$$

$$Ex_R = \frac{\int_0^{RRS_{\max}} RRS \cdot Pr[RRS] \cdot dRRS}{\int_0^{RRS_{\max}} RRS \cdot dRRS} \quad (5)$$

where

$$R_U(t) = \sum_{i=1}^{cars} MnAP_i(t) \quad (6)$$

$$R_D(t) = \sum_{i=1}^{cars} MxAP_i(t) \quad (7)$$

$$R_R(t) = \sum_{i=1}^{cars} RsRP_i(t) \quad (8)$$

The aggregator costs from performing V2G come from the wholesale cost of energy which is delivered to the EVs and the battery degradation associated from discharging. These costs are shown in (9).

$$\begin{aligned}
 C = & \sum_i \sum_t (E [FP_i(t)] \cdot P(t)) \\
 & + \sum_i \sum_t \left(\frac{DC_i \cdot E [FP_i^-(t)]}{Ef_i} \right).
 \end{aligned} \quad (9)$$

The first term in (9) is zero unless $E [FP_i(t)] > 0$. The second term is also zero unless $E [FP_i^-(t)] > 0$.

The expected value of the reduction portion of the final power draw and the degradation costs are given by

$$\begin{aligned}
 E [FP_i^-(t)] = & POP_i(t) - MnAP_i(t) \\
 & \cdot Ex_U - RsRP_i(t) \cdot Ex_R
 \end{aligned} \quad (10)$$

$$DC_i = 0.042 \left(\frac{BatC_i}{5000} \right) + \frac{1 - Ef_i^2}{Ef_i} Mk. \quad (11)$$

$E [FP_i^-(t)]$ is used when calculating the cost of battery degradation because it is a more conservative estimate of discharge rate than what is given by $E [FP_i(t)]$. The first term in (11) is the battery replacement cost normalized by the battery replacement cost used in [18], [19]. This normalized cost is multiplied by the degradation cost of a kWh of energy throughput that was found in the same studies. While this value is chemistry specific, it can be adapted for any chemistry that would be used. However, characterizing the different battery chemistry degradation costs is beyond the scope of this work and though the value of the degradation will change with chemistry, the formulation will not. Since this uses the average cost of V2G dispatch calculated in [18], [19], the depth of discharge effects are ignored. These can be included, however, by breaking the constant slope into a piecewise linear slope.

The second term of the degradation cost is a balancing term multiplied by the aggregator price of energy to account for the differences in energy delivered to and taken from the battery compared to what is measured at the meter. For example, if the aggregator charges 4 kWh into the battery, with a 90% charging efficiency then the customer is billed for $4/0.9 = 4.44$ kWh. If the aggregator then discharges 4 kWh from the battery with a 90% discharge efficiency, then the customer is paid for $4 \cdot 0.9 = 3.6$ kWh. Charging another 4 kWh hours to the battery results in the customer being charged for 4.44 kWh again. In this way the aggregator could increase its profits from energy sales by charging and discharging the battery. The second term

in the degradation costs, however, balances this so that there is no incentive for the aggregator to overcharge the customers.

The constraints on the optimization are battery capacity limits, charging station maximum current, customer-defined minimum SOC limits for driving purposes, and system loading limits. While customer preferences on SOC vary, a safe assumption is that before the morning commute, at the start of the aggregator scheduling day, the customer requires that the SOC is enough for the morning and evening commute. Additionally, after the morning commute, the SOC must at least always be greater than that required for the evening commute as given in (20). Another relatively safe assumption is that the customer requires the car to be at least 99% charged by the morning hours as given in (17).

This optimization problem can be formulated as a linear program with the decision variables being the POP , $MxAP$, $MnAP$, and $RsRP$ of each EV. In order to eliminate the conditions on some of the cost terms, the epigraph variable Deg is introduced for each EV. Since an EV can depart unexpectedly during a scheduling period, it is necessary for the aggregator to under schedule capacity and then over dispatch when the EV departs. This is done to compensate for the lost capacity. The compensation factor is given by

$$Comp_i(t) = 1 + \frac{Dep_i(t)}{1 - Dep_i(t)}. \quad (12)$$

In this study, $Comp_i$ is treated deterministically for large numbers of EVs, which is allowable for groups of 10 000 or more [16]. Also due to the departures of EVs, the aggregator's expected profits each hour will be decreased to only the number of EVs remaining. The percentage of EVs remaining to perform V2G in a particular hour is given by

$$EVPer(t) = \begin{cases} 1 - \sum_{time=1}^t \sum_i Dep_i(time) & \text{if } t < T_{trip,i} \\ 1 - \sum_{time=T_{trip,i}}^t \sum_i Dep_i(time) & \text{if } t \geq T_{trip,i}. \end{cases} \quad (13)$$

The final problem formulation is

$$\underset{POP_i(t), MxAP_i(t), MnAP_i(t), RsRP_i(t), Deg_i(t)}{\text{maximize}} \quad In - C \quad (14)$$

subject to:

$$\left(\sum_{t=1}^{time} (E[FP_i(t)] \cdot Comp_i(t) + \rho_i(t)) \cdot Ef_i + SOC_{I,i} - Trip_i(time) \right) \leq M_{Ci} \quad \forall i, time \quad (15)$$

$$\left(\sum_{t=1}^{time} (E[FP_i(t)] \cdot Comp_i(t) + \rho_i(t)) \cdot Ef_i + SOC_{I,i} - Trip_i(time) \right) \geq 0 \quad \forall i, time \quad (16)$$

$$\left(\sum_{t=1}^T (E[FP_i(t)] \cdot Comp_i(t) + \rho_i(t)) \cdot Ef_i + SOC_{I,i} - Trip_i(T) \right) \geq 0.99M_{Ci} \quad \forall i \quad (17)$$

$$(MxAP_i(1) + POP_i(1)) \cdot Comp_i(1) \cdot Ef_i + SOC_{I,i} \leq M_{Ci} \quad \forall i \quad (18)$$

$$\left(\begin{array}{l} (POP_i(1) - MnAP_i(1) - RsRP_i(1) + \rho_i(1)) \\ \cdot Comp_i(1) \cdot Ef_i + SOC_{I,i} \end{array} \right) \geq 0 \quad \forall i \quad (19)$$

$$\left(\begin{array}{l} (POP_i(1) - MnAP_i(1) - RsRP_i(1) + \rho_i(1)) \\ \cdot Comp_i(1) \cdot Ef_i + SOC_{I,i} \end{array} \right) \geq Trip_i \quad \forall i \quad (20)$$

$$(MxAP_i(t) + POP_i(t)) \cdot Comp_i(t) \leq MP_i(t) \quad \forall i \quad (21)$$

$$MnAP_i(t) \leq POP_i(t) + MP_i(t) \quad \forall i \quad (22)$$

$$RsRP_i(t) \leq POP_i(t) + MP_i(t) - MnAP_i(t) \quad \forall i \quad (23)$$

$$MxAP_i(t) \geq 0 \quad \forall i \quad (24)$$

$$MnAP_i(t) \geq 0 \quad \forall i \quad (25)$$

$$RsRP_i(t) \geq 0 \quad \forall i \quad (26)$$

$$POP_i(t) \geq -MP_i(t) \quad \forall i \quad (27)$$

$$Deg_i(t) \geq 0 \quad \forall i \quad (28)$$

$$Deg_i(t) \geq DC_i \cdot E[FP_i^-(t)] \cdot \frac{Comp_i(t)}{Ef_i} \quad \forall i \quad (29)$$

$$\sum_i^{cars} POP_i(t) \leq \frac{MxL - L(t)}{MxL - MnL} \sum_i^{cars} MP_i(t) \quad \forall t \quad (30)$$

with

$$In = \sum_t \left(\left(\begin{array}{l} P_{RU}(t) \cdot R_U(t) + P_{RD}(t) \cdot R_D(t) \\ + P_{RR}(t) \cdot R_R(t) \end{array} \right) \cdot EVPer(t) \right) + Mk \sum_i \sum_t (E[FP_i(t)] \cdot EVPer(t)) \quad (31)$$

$$C = \sum_i \sum_t (E[FP_i(t)] \cdot EVPer(t) \cdot P(t)) + \sum_i \sum_t (Deg_i(t)) \quad (32)$$

$$\rho_i(t) = \left(\frac{Deg_i(t)}{DC_i} \right) \frac{1 - Ef_i^2}{Ef_i}. \quad (33)$$

The term $\rho_i(t)$ is to account for the energy discharged from the battery due to the discharge efficiency and is similar to the balancing term in the aggregator degradation costs. The system loading constraint (30) ensures that the combined charging of the EVs does not add to the forecasted system peak load as well as limiting how much additional load can be added during other hours. The necessity of this constraint is discussed in greater detail in [3], [20]. Careful examination of the problem formulation reveals that it is linear with respect to all of the decision variables and is hence a convex linear program.

Some EV owners are insensitive to price, however, and will sometimes require to charge at peak load. This can be handled under (30) by discharging from other EVs that have sufficient capacity and time to supply extra power during the peak load period. Since peak load often occurs during peak price, many of the EVs will be discharging anyways. Price insensitive customers may not desire to participate in V2G either, in which case they may be charged real time prices by the aggregator.

Constraint (30), however, does not solve distribution system overloads and poor voltage profiles as a result of EV charging [8]. Some methods to solve these problems include charging with the objective of minimizing system losses, minimizing load variance, or maximizing load factors [21], [22]. Those methods

that are convex problems can be integrated into this formulation by adapting the objective functions to additional constraints. Such constraints would be imposed by the distribution system operator for specific feeders. This is possible for minimizing load variance and maximizing load factor. Such adaptation, however, is beyond the scope of this work. If no distribution system constraints are imposed, the final EV charging profiles may need to be approved by the distribution system operator. For very low penetrations of EVs with low clumping, the optimal charging profiles should not be overly problematic since (30) prevents charging coincident with peak loads.

This formulation assumes that the aggregator has accurate information on the EV driving patterns and battery SOC while charging. This is possible with existing technology using several methods. One method relies on machine learning of historical charge amounts and times to estimate the driving pattern and initial battery SOC to a high degree of certainty. This is especially effective with commuter cars. The changes in SOC can be calculated from the energy dispatched to the EV during the charging period. Another method leverages the advanced connectivity of EVs. Newer EVs have smart phone connectivity that allows the owner to see the SOC as well as set the desired time to finish charging [23]. This information could be provided to the aggregator through another smart phone app to be used in the optimization. A combination of these two methods is also possible.

IV. ANCILLARY SERVICES ALGORITHMS

Once the capacities of each ancillary service are bid, the EVs must then respond to the dispatch signals received from the system. Ancillary services can be performed by EVs through varying their charging rates around the POP [11], [12]. The POP can be either positive or negative. The dispatch for regulation up or responsive reserves can be a reduction in charging, an increase in discharging, or a combination of the two. Similarly, the regulation down dispatch is a reduction in the discharge rate, an increase in the charging rate, or a combination of the two. These algorithms work sequentially. For a given regulation and responsive reserve signal, the EV dispatch to follow the regulation signal is first computed, and then the resulting power draw of the EV is used to calculate its response to the responsive reserve signal. The aggregator receives the signals from the system and then calculates each EV's portion of the response to the signal, and sends that resulting signal to the EVs. These calculations occur in fractions of a second. Since the constraints ensure that there is almost always adequate capacity to perform the dispatch there is no dispatch of one service at the expense of the other. Since there are no conflicts of service dispatch priority, the dispatches to the two services could also be independently computed in parallel and added together yielding the same result. The regulation and responsive reserves algorithms are shown in Figs. 1 and 2. A graphical depiction of regulation and responsive reserves capacities and dispatch is shown in Fig. 3.

V. SIMULATION

The algorithms are simulated over a three month period on a hypothetical group of 10 000 EVs used by commuters in the Houston area. This is a sufficiently large number to determine

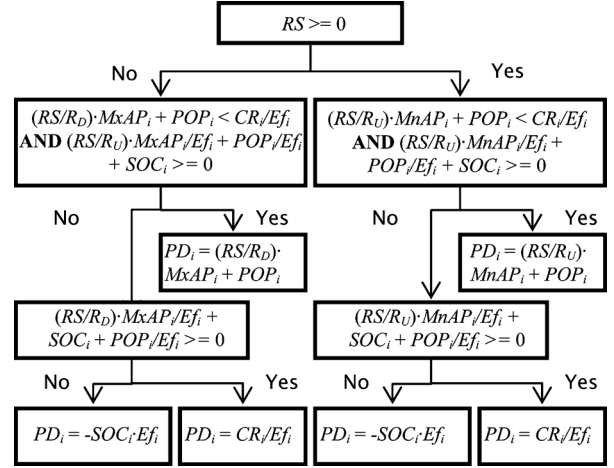


Fig. 1. Regulation dispatch algorithm for an EV.

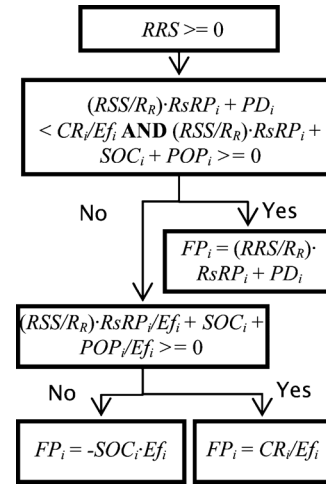


Fig. 2. Responsive reserves dispatch algorithm for an EV.

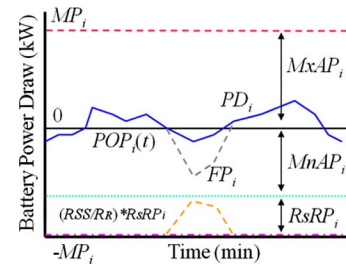


Fig. 3. Graphical depiction of a charging profile showing variable meanings.

the power capacities to a high degree of certainty [16]. Since battery degradation costs are the most limiting factor to the profitability of bidirectional V2G, three different replacement costs are simulated, \$200/kWh, \$400/kWh, and \$800/kWh, which is in the range considered in [18], [19]. The system is simulated in Matlab and the optimizations are solved using CVX [24]. A simulation day begins at 6 A.M.. The battery SOC from the previous day is assigned as the initial SOC for the current day. The study system uses net load, ancillary services deployments, and market prices for energy, regulation, and responsive reserves from available ERCOT archives for the period of July 21, 2010 to October 20, 2010 [25]. Ancillary services bid stacks are also taken from the archives over the same period and are used to measure the impact of V2G ancillary services on the

market prices of those services. The ancillary services deployments are given in five minute increments, which is adequate for measuring energy delivered to the EV [3]. The net load and prices are those from the Houston congestion management zone. Hourly net load forecasts and schedules are generated using the method in [26], which adds an error to the actual hourly load average. Day-ahead load forecasts are the actual load forecasts used in the ERCOT system [25], and the day-ahead price forecasts are generated to statistically match the error distributions found in [27]. Day-ahead ancillary services prices are forecasted using a given-hour persistence forecast method. This method assumes that the price for a given hour tomorrow will be the same as it was for the given hour today. Mean absolute percentage errors of this forecast method over the simulation time period were less than 25% for each of the services bid.

Five different cars that are currently available for purchase or lease are used to construct a hypothetical group for use in the simulations. These are Tesla Roadster, Think City, BMW MINI-E, Mitsubishi i-MiEV, and the Nissan Leaf. Of this group, it is assumed that 5% of the vehicles are Tesla Roadsters, 20% are Think Cities, 25% are i-MiEVs, 20% are MINI-Es, and 30% are Leafs. EV charging and discharging efficiencies are assumed to be 90%. The home and workplace chargers are assumed to be rated at 240 V, 30 A [28], [29]. Though only battery electric vehicles are used in this study, the algorithm will work equally well with groups that include plug-in hybrids. Plug-in hybrids may also have the ability to use their engines to produce electricity when the energy price is sufficiently high. For this case, fuel costs and constraints would need to be added to the formulation. The driving efficiencies, battery capacities, and other EV specifications are given in [30]–[35].

Using data from the 2009 National Highway Travel Survey [36] for urban Texas households, 100 different weekday and 100 weekend driving profiles are constructed. The EVs are randomly assigned driving profiles in groups of 100. Each driving profile has unique morning commute start and end times, evening commute start and end times, and commute distances. Evening commute times range from 4 P.M. to 7 P.M. and morning commute times are between 6 A.M. and 9 A.M.. Weekend first daily trips occur between 11 A.M. and 2 P.M. with the evening trips occurring between 5 P.M. and 8 P.M.. Each hour that an EV is traveling, it is unavailable to participate in V2G. All other times the EVs are assumed plugged in and available.

Each hour of EV availability has an associated unplanned departure probability. Such probabilities can be calculated over time by examining driving behaviors. Since such detailed data is not available in the NHTS set, the probabilities are estimated to be a 10% chance of early departure during the weekday working hours, and a 20% chance of an extra trip during the evening hours. On weekends, the unexpected departure probability is 20% throughout the day. From 3 A.M. to 6 A.M., it is assumed that all EVs are plugged in and available with a 0% chance of unexpected departure. Using these probabilities, a set of departures was generated for each 5 min period in the simulation set for consistency between the different simulation trials.

The aggregator rate of energy charged to the consumer is \$0.01/kWh. All of the degradation costs are paid to the customer on a monthly basis. The aggregator pays the wholesale cost of energy on the spot market and receives all revenues from selling

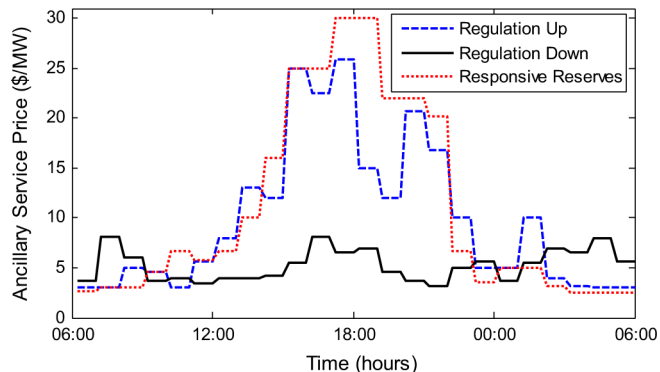


Fig. 4. Hourly ancillary services prices for August 2, 2010.

energy and ancillary services. It is assumed that communication from the aggregator to the EVs is done on existing smart grid communication channels [3].

This study highlights the possibilities for profits, ancillary capacities, and peak load shaving for large numbers of EVs if they are equipped for bidirectional power flow and are optimally aggregated. This is important to know for system planners who must look several years into the future when making decisions about infrastructure. Since Houston is a city that has a large rollout of EV charging stations under the eVgo network [37], it is not unrealistic to assume that mass V2G could also be adopted there.

VI. RESULTS

For each day, the optimization is run each hour to find the optimal schedule for that hour. EV dispatches in response to the system ancillary services signals are recorded every five minutes, which changes the level of the battery SOC. Each hour, the new SOC is used when formulating the optimal dispatch for the remaining hours in the dispatch period. Hourly load and prices forecast errors are reduced by 4% to simulate improved forecasting with shorter time horizons.

A. Charging Profiles

Profiles of the POP and ancillary services capacities relative to the POP are compared for August 2, 2010. This day was chosen because the variations in energy and ancillary services prices highlight the merits of the algorithm as well as the impact of different battery degradation costs. Hourly ancillary services prices for the day are shown in Fig. 4, and hourly energy prices are shown in Fig. 5. It can be seen in Fig. 5 that the peak price is over 10 times as high as the minimum price. Such a differential is high enough to compensate for the battery degradation and additional losses from a bulk discharge.

The charging and the ancillary services profiles are shown in Figs. 6–8 for the three different battery replacement costs in Section V. The main difference between the three is the amount of energy sold at the daily high price at 4:00 P.M. With a replacement cost of \$200/kWh, nearly 50 MW of energy is sold to the grid. At \$400/kWh, the amount sold is closer to 40 MW. At \$800/kWh, less than 20 MW are sold. The amount of regulation up capacity that is sold also reduces as the battery replacement costs increase. Generally, during the working hours and for all replacement costs, the POP is slightly positive with large amounts of regulation up capacity sold. At 2 P.M., when

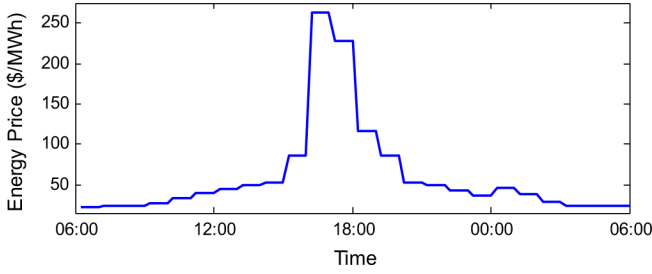


Fig. 5. Hourly energy price for August 2, 2010.

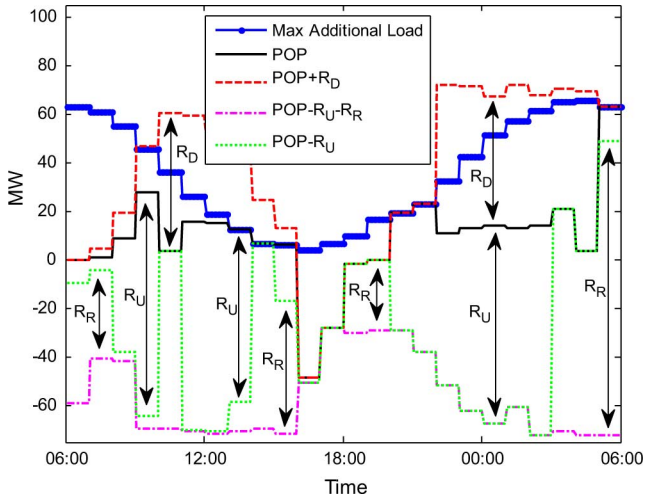


Fig. 6. Charging profile, ancillary services capacities and system load constraint for the algorithm with battery replacement costs of \$200/kWh.

the price of responsive reserves is greater than that of regulation up, only responsive reserves and a small amount of regulation down are sold. At these hours, the system load constraint prevents the POP from being raised to sell more capacity of responsive reserves. The time of the peak system load occurs at the peak price and so energy is discharged from the batteries which helps shave the peak. In the evening and night hours, the POP is slightly positive again with higher capacities of regulation down being sold. This is due to the high relative price of regulation down and because the batteries need to be charged to 99%. The last few hours, no regulation up is sold as its expected value of dispatch is higher than that of responsive reserves and battery charging has a higher priority. The last hour the POP is set at the maximum allowed to finish topping off the batteries.

These charging profiles show that the optimal behavior seldom sets the POP at zero, usually bids asymmetric capacities of regulation, and often biases the POP while selling ancillary services.

B. Quarterly Results Summary

Examining the algorithms' performance over the simulated quarter reveals their benefits as well as the impact of the costs of battery replacement. The quarterly aggregator profits and degradation costs are shown in Fig. 9. It is clear that the profits to the aggregator are higher when the degradation cost is lower. This is because the degradation payments to the customer are lower. Also, if the battery cycling is reduced, there is less capacity to sell ancillary services, as shown in Fig. 10. In all cases the yearly aggregator profits can be extrapolated from the quar-

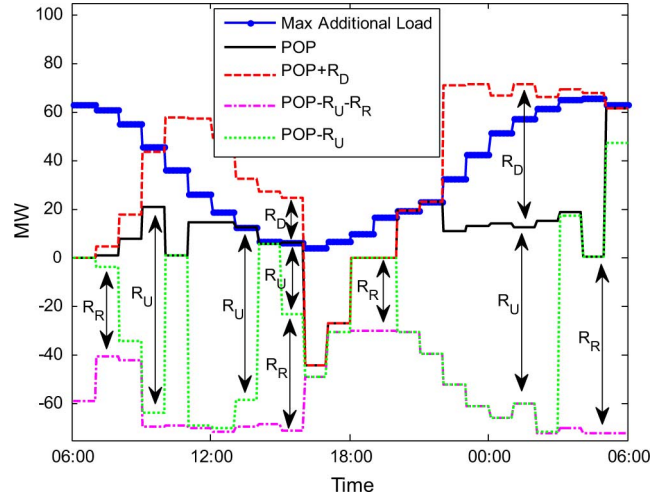


Fig. 7. Charging profile, ancillary services capacities and system load constraint for the algorithm with battery replacement costs of \$400/kWh.

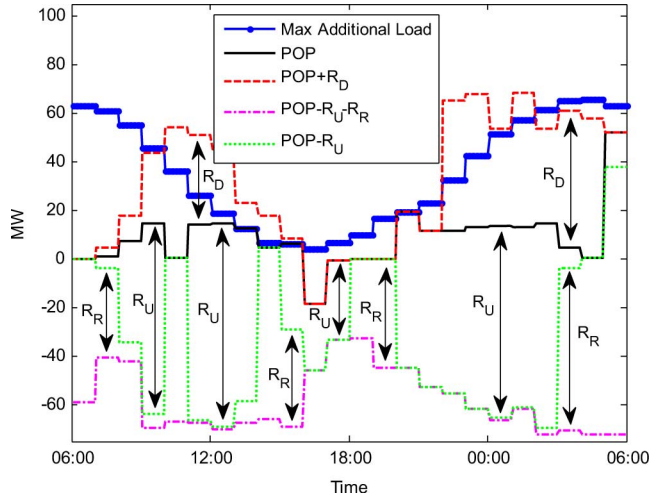


Fig. 8. Charging profile, ancillary services capacities and system load constraint for the algorithm with battery replacement costs of \$800/kWh.

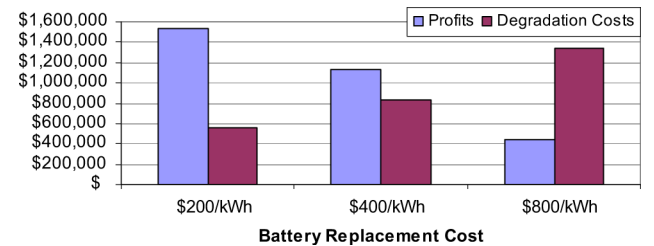


Fig. 9. Quarterly aggregator profits and degradation costs for different battery replacement costs.

terly results to be over \$1 200 000. With degradation costs of only \$200/kWh the yearly profits are over \$6 000 000.

The system benefits from the implementation of the algorithms are also significant. From Fig. 10 it is clear that the system gains tens of MW of regulation and reserves capacity which can be used for balancing intermittent renewable energy sources. This, however, is a small percentage of the average capacity requests of 800 MW of each regulation up and down, and 2300 MW of responsive reserves [25]. System ancillary services prices also reduced by approximately 7%–8% depending on the replacement cost of the battery. Additionally, the system peak load is, on average, reduced through the dis-

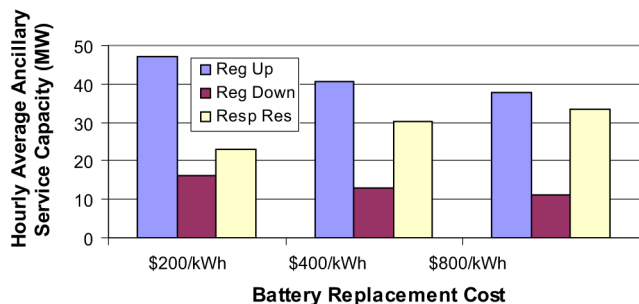


Fig. 10. Hourly average ancillary service capacity bid for different battery replacement costs. Resp Res represents responsive reserves.

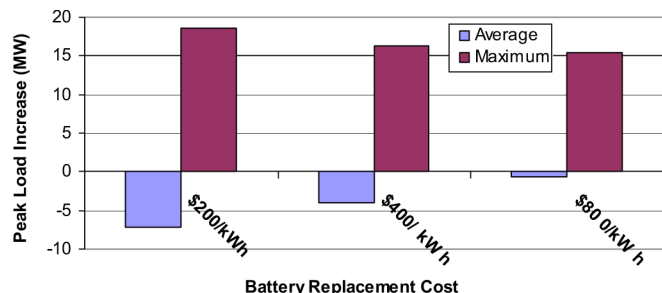


Fig. 11. Average and maximum peak load increase for different battery replacement costs.

charge of energy at high prices as shown in Fig. 11. It can also be seen that the lower the battery replacement costs, the greater the peak shaving. Though the maximum peak load increase during the quarter is over 15 MW, this is only due to forecast errors when setting the load constraint.

The customers receive the benefit of being able to charge their EVs for only \$0.01/kWh, which is lower than the lowest retail rates in the United States. This is a significant market-based financial incentive which can aid in hastening the adoption of EVs. Also, due to the minimum SOC constraint for the last hour, the SOC is always over 98% for the whole group. The only reason it is below the minimum 99% is due to regulation up and responsive reserves dispatches greater than the expected values.

C. Cost-Benefit Analysis

A simple cost-benefit analysis is performed to see the maximum amount that the aggregator or the system would be willing to pay for the capital costs of retrofitting the EVs for bidirectional capability. The net present value (NPV) is calculated for each EV by extrapolating the net revenues from energy and ancillary services to one year and using the NPV formula in [17] for the expected life of the car. If the risk free rate is assumed to be 1% and the expected life of the car is 10 years the NPV is at most \$6,082.80 per car and is strongly a function of battery replacement costs. The NPVs are shown in Table I. These values, however, are only valid if the price of ancillary services remains the same year to year, which is unlikely if EV adoption increases dramatically.

VII. DISCUSSION

It is clear that optimal scheduling of V2G energy and ancillary services provides significant benefits to all involved. However, there are several challenges in the implementation that must be addressed. Currently, none of the consumer EVs that

TABLE I
NET PRESENT VALUE OF V2G PEAK SHAVING AND ANCILLARY SERVICES

Battery Cost	\$200/kWh	\$400/kWh	\$800/kWh
NPV Per Car	\$6,082.80	\$4,433.90	\$1,540.78

are being produced has the capability to provide energy back to the grid. There is also the problem of protection at the point of interconnection. These two issues will require aftermarket hardware, the cost of which may not be justified by the NPV of V2G per car. Additionally, such aftermarket retrofits will most likely void the manufacturer warranties on the batteries [3]. Though the customers will be compensated for the cost of degradation, they will have to purchase replacement batteries more frequently, which is an inconvenience they may not want to deal with [38].

Nevertheless, there are at least two cases where these algorithms can be implemented which are not hindered by the challenges listed above. The first is the case of utility installed community energy storage (CES). This is often installed with the intent of deferring infrastructure upgrades due to short term overloads of feeders and transformers. Such discharge would be analogous to the daily trips. The rest of the time, the utility could optimally schedule their distributed CES using these algorithms.

The other case is that of electric delivery trucks and vans used for businesses. Such heavy duty EVs are often desired to come with V2G capability for use as a backup power source at warehouses and businesses [39]. In this case, all interconnection and protection issues would already have been installed for the backup system. From a business prospective, if it is more profitable to replace the battery more frequently due to V2G operation, it will not be an inconvenience, but a welcome opportunity.

VIII. CONCLUSION

In this work an optimal scheduling algorithm for V2G energy and ancillary services is formulated. This algorithm simultaneously schedules energy sales and multiple ancillary services. In addition, algorithms for performing the V2G ancillary services are developed. Simulation on the Houston area of the ERCOT system using a group of 10 000 commuter EVs show that the algorithms offer significant financial benefits to customers and aggregators for different battery replacement costs. Additional system flexibility as well as peak load reductions are also observed, which can aid the system in integrating additional intermittent renewable energy sources. Though there are several challenges that must be overcome before V2G can be fully implemented at a commuter EV level, the cases of utility owned CES and heavy duty commercial EVs are not hindered by those challenges.

REFERENCES

- [1] W. Kempton and J. Tomic, "Vehicle-to-grid power implementation: From stabilizing the grid to supporting large-scale renewable energy," *J. Power Sources*, vol. 144, no. 1, pp. 280–294, Jun. 2005.
- [2] W. Kempton and J. Tomic, "Vehicle-to-grid power fundamentals: Calculating capacity and net revenue," *J. Power Sources*, vol. 144, no. 1, pp. 268–279, Jun. 2005.
- [3] E. Sortomme and M. A. El-Sharkawi, "Optimal charging strategies for unidirectional vehicle-to-grid," *IEEE Trans. Smart Grid*, vol. 2, no. 1, pp. 131–138, 2011.

- [4] C. Guille and G. Gross, "A conceptual framework for the vehicle-to-grid (V2G) implementation," *Energy Policy*, vol. 37, no. 11, pp. 4379–4390, 2009.
- [5] C. Quinn, D. Zimmerle, and T. H. Bradley, "The effect of communication architecture on the availability, reliability, and economics of plug-in hybrid electric vehicle-to-grid ancillary services," *J. Power Sources*, vol. 195, no. 5, pp. 1500–1509, 2010.
- [6] A. Brooks, E. Lu, D. Reicher, C. Spirakis, and B. Wehl, "Demand dispatch," *IEEE Power Energy Mag.*, vol. 8, no. 3, pp. 20–29, 2010.
- [7] S. Han and K. Sezaki, "Development of an optimal vehicle-to-grid aggregator for frequency regulation," *IEEE Trans. Smart Grid*, vol. 1, no. 1, pp. 65–72, 2010.
- [8] J. A. P. Lopes, F. J. Soares, and P. M. R. Almeida, "Integration of electric vehicles in the electric power system," *Proc. IEEE*, vol. 99, no. 1, pp. 168–183, 2011.
- [9] M. Gallus, S. Koch, and G. Andersson, "Provision of load frequency control by phev's, controllable loads, and a co-generation unit," *IEEE Trans. Ind. Electron.*, unpublished.
- [10] J. Tomic and W. Kempton, "Using fleets of electric-drive vehicles for grid support," *J. Power Sources*, vol. 168, no. 2, pp. 459–468, 2007.
- [11] A. Brooks, "Vehicle-to-grid demonstration project: Grid regulation ancillary service with a battery electric vehicle," California Air Resources Board, Final Rep., 2002.
- [12] W. Kempton, V. Udo, K. Huber, K. Komara, S. Letendre, S. Baker, D. Brunner, and N. Pearre, "A test of vehicle-to-grid (V2G) for energy storage and frequency regulation in the PJM system," Univ. Delaware, Newark, Rep., 2008.
- [13] Y. Ota, H. Taniguchi, T. Nakajima, K. M. Liyanage, K. Shimizu, T. Masuta, J. Baba, and A. Yokoyama, "Effect of autonomous distributed vehicle-to-grid for ubiquitous power grid and its effect as a spinning reserve," *J. Int. Council Electr. Eng.*, vol. 1, no. 2, pp. 214–221, 2011.
- [14] J. R. Pillai and B. Bak-Jensen, "Integration of vehicle-to-grid in the western danish power system," *IEEE Trans. Sustainable Energy*, vol. 2, no. 1, pp. 12–19, 2011.
- [15] Y. Hanai, K. Yoshimura, J. Matsuki, and Y. Hayashi, "Load management using heat-pump water heater and electric vehicle battery charger in distribution system with PV," *J. Int. Council Electr. Eng.*, vol. 1, no. 2, pp. 207–213, 2011.
- [16] D. Dallinger, D. Krampe, and M. Wietschel, "Vehicle-to-grid regulation reserves based on a dynamic simulation of mobility behavior," *IEEE Trans. Smart Grid*, vol. 2, no. 2, pp. 302–313, 2011.
- [17] N. Rotering and M. Ilic, "Optimal charge control of plug-in hybrid electric vehicles in deregulated electricity markets," *IEEE Trans. Power Syst.*, vol. 26, no. 3, pp. 1021–1029, 2011.
- [18] S. B. Peterson, J. F. Whitacre, and J. Apt, "The economics of using plug-in hybrid electric vehicle battery packs for grid storage," *J. Power Sources*, vol. 195, no. 8, pp. 2377–2384, 2010.
- [19] S. B. Peterson, J. Apt, and J. F. Whitacre, "Lithium-ion battery cell degradation resulting from realistic vehicle and vehicle-to-grid utilization," *J. Power Sources*, vol. 195, no. 8, pp. 2385–2392, 2010.
- [20] T. Markel, M. Kuss, and P. Denholm, "Communication and control of electric vehicles supporting renewables," in *Proc. 2009 IEEE Veh. Power Propulsion Syst. Conf.*, Sep. 2009, pp. 1–8.
- [21] K. Clement-Nyns, E. Haesen, and J. Driesen, "The impact of charging plug-in hybrid electric vehicles on a residential distribution grid," *IEEE Trans. Power Syst.*, vol. 25, no. 1, pp. 371–380, 2010.
- [22] E. Sortomme, M. Hindi, S. D. J. MacPaherson, and S. S. Venkata, "Coordinated charging of plug-in hybrid electric vehicles to minimize distribution system losses," *IEEE Trans. Smart Grid*, vol. 2, no. 1, pp. 198–205, 2011.
- [23] Nissan LEAF Electric Car, FAQ: Features, Aug. 10, 2010 [Online]. Available: <http://www.nissanus.com/leaf-electric-car/index?dcp=ppn.39666654.&dcc=0.216878497#/leaf-electric-car/faq/list/features>
- [24] M. Grant and S. Boyd, CVX: Matlab Software for Disciplined Convex Programming, Version 1.21, Feb. 2011 [Online]. Available: <http://cvxr.com/cvx>
- [25] Electric Reliability Council of Texas, Market Information, Aug. 20, 2010 [Online]. Available: <http://www.ercot.com/mktinfo/>
- [26] Y. Makarov, S. Lu, B. McManus, and J. Pease, "The future impact of wind on bpa power system ancillary services," in *Proc. Transm. Distrib. Conf. Expo.*, Apr. 2008, pp. 1–5.
- [27] N. Amjady, "Day-ahead price forecasting of electricity markets by a new fuzzy neural network," *IEEE Trans. Power Syst.*, vol. 21, no. 2, pp. 887–896, 2006.
- [28] AeroVironment EV Solutions, Electric Vehicle Home Charging Dock, Nov. 14, 2010 [Online]. Available: http://evsolutions.avinc.com/uploads/products/2_AV_EVSE-RS_B2B_061110_retail_charging.pdf
- [29] AeroVironment EV Solutions, Commercial and Public Electric Vehicle Charging, Nov. 14, 2010 [Online]. Available: http://evsolutions.avinc.com/uploads/products/1_AV_EVSE-CS_061010_fleet_ac.pdf
- [30] G. Berdichevsky, K. Kely, J. B. Straubel, and E. Toomre, Tesla Motors, The Tesla Roadster Battery System, Dec. 5, 2009 [Online]. Available: http://www.teslamotors.com/display_data/teslaroadster_specsheet.pdf
- [31] Tesla Motors, Tesla Roadster Spec Sheet, Dec. 5, 2009 [Online]. Available: http://www.teslamotors.com/display_data/teslaroadster_specsheet.pdf
- [32] Think, Technical Data, Dec. 5, 2009 [Online]. Available: <http://thinkev.com/The-THINK-City/Specifications/Technical-data>
- [33] MINI, MINI-E Specifications, Dec. 5, 2009 [Online]. Available: <http://www.miniusa.com/minie-usa/pdf/MINI-E-spec-sheet.pdf>
- [34] Mitsubishi Motors, Mitsubishi Motors to Bring New-Generation EV I-MiEV to Market, Dec. 5, 2009 [Online]. Available: <http://media.mitsubishi-motors.coAm/pressrelease/e/products/detail1940.html>
- [35] Nissan Zero Emission Website, Leaf Specs, May 1, 2010 [Online]. Available: <http://www.nissan-zeroemission.com/EN/LEAF/specs.html>
- [36] Federal Highway Administration, National Household Travel Survey, Aug. 1, 2010 [Online]. Available: <http://nhts.ornl.gov/>
- [37] eVgo, The Network, Jun. 20, 2011 [Online]. Available: https://www.evgo.com/The_Network/
- [38] B. K. Sovacool and R. F. Hirsh, "Beyond batteries: An examination of the benefits and barriers to plug-in hybrid electric vehicles (PHEVs) and a vehicle-to-grid (V2G) transition," *Energy Policy*, vol. 37, no. 3, pp. 1095–1103, 2009.
- [39] G. McBride, "EV charging is a demand response opportunity," in *Proc. DistributeCH 2011*, pp. 1–19.



Mr. Sortomme is a corecipient of the 2010 UW Department of Electrical Engineering Chair's Award.



Eric Sortomme (S'08) received the B.S. degree in electrical engineering (*magna cum laude*) from Brigham Young University, Provo, UT, in 2007 and the Ph.D. degree from the University of Washington, Seattle, in 2011.

His employment experience includes internships with Wavetronix LLC and Puget Sound Energy. He has authored or coauthored a plethora of additional technical publications. His research interests include smart grid technologies, including microgrids and vehicle-to-grid, and wind power integration.

Mohamed A. El-Sharkawi (F'95) received the Ph.D. degree in electrical engineering from the University of British Columbia, Vancouver, Canada, in 1980.

In 1980 he joined the University of Washington, Seattle, as a Faculty Member where he is presently a Professor of Electrical Engineering. He also served as the Associate Chair and the Chairman of Graduate Studies and Research. He has been the Founding Chairman of numerous IEEE task forces and working groups and subcommittees and published over 200

papers and book chapters in his research areas.